

1 **Disentangling residence time and temperature sensitivity** 2 **of microbial decomposition in a global soil carbon model**

3

4 **J.-F. Exbrayat^{1,2}, A. J. Pitman¹ and G. Abramowitz¹**

5

6 [1]{ARC Centre of Excellence for Climate System Science and Climate Change Research
7 Centre, University of New South Wales, Sydney, New South Wales, Australia}

8 [2]{School of GeoSciences and National Centre for Earth Observation, University of
9 Edinburgh, Edinburgh, UK}

10 Correspondence to: J.-F. Exbrayat (j.exbrayat@ed.ac.uk)

11

12 **Abstract**

13 Recent studies have identified the first-order representation of microbial decomposition as a
14 major source of uncertainty in simulations and projections of the terrestrial carbon balance.
15 Here, we use a reduced complexity model representative of current state-of-the-art models of
16 soil organic carbon decomposition. We undertake a systematic sensitivity analysis to
17 disentangle the effect of the time-invariant baseline residence time (k) and the sensitivity of
18 microbial decomposition to temperature (Q_{10}) on soil carbon dynamics at regional and global
19 scales. Our simulations produce a range in total soil carbon at equilibrium of ~ 592 to 2745 Pg
20 C which is similar to the ~ 561 to 2938 Pg C range in pre-industrial soil carbon in models
21 used in the fifth phase of the Coupled Model Intercomparison Project. This range depends
22 primarily on the value of k , although the impact of Q_{10} is not trivial at regional scales. As
23 climate changes through the historical period, and into the future, k is primarily responsible
24 for the magnitude of the response in soil carbon, whereas Q_{10} determines whether the soil
25 remains a sink, or becomes a source in the future mostly by its effect on mid-latitudes carbon
26 balance. If we restrict our simulations to those simulating total soil carbon stocks consistent
27 with observations of current stocks, the projected range in total soil carbon change is reduced
28 by 42% for the historical simulations and 45% for the future projections. However, while this
29 observation-based selection dismisses outliers it does not increase confidence in the future

30 sign of the soil carbon feedback. We conclude that despite this result, future estimates of soil
31 carbon, and how soil carbon responds to climate change should be constrained by available
32 observational data sets.

33

34 **1 Introduction**

35 There is a 6-fold range in the amount of carbon stored in the soil in simulations conducted as
36 part of the fifth phase of the Coupled Model Intercomparison Project (CMIP5; Taylor et al.,
37 2012). This 6-fold range, identified by Todd-Brown et al. (2013), is consistent with results
38 from the recent model intercomparison projects such as the Coupled Climate-Carbon Cycle
39 Model Intercomparison Project (C⁴MIP; Friedlingstein et al., 2006). The analysis of carbon
40 stores in both C⁴MIP and CMIP5 have focused on the prediction of terrestrial and soil carbon
41 through time. In addition to demonstrating the large differences in carbon stocks (Todd-
42 Brown et al., 2013), they have also highlighted large inter-model differences in global and
43 regional land-atmosphere carbon (C) fluxes (e.g. Friedlingstein et al., 2006, 2014). This lack
44 of agreement between simulations exists in fully coupled models (e.g. C⁴MIP and CMIP-5)
45 but can also be found if sources of uncertainty are narrowed by relying on one weather
46 dataset to drive multiple land models (Friend et al., 2013; Nishina et al., 2014), or by using
47 one land model driven by multiple climate projections (Ahlström et al., 2013).

48 In these previous studies, critical uncertainties have been identified in the microbial
49 decomposition of soil organic C and the associated release of CO₂ via heterotrophic
50 respiration (R_h). This is despite all the current state-of-the-art global soil C models relying on
51 a similar representation of decomposition as a first-order process (see Exbrayat et al., 2013b;
52 Nishina et al., 2014; Todd-Brown et al., 2013). This conceptualization describes
53 decomposition and R_h as proportional to the availability of organic matter. The decay rate (or
54 R_h per unit of soil C) is modified based on an environmental scalar that intends to mimic the
55 dynamical response of microbial biomass to soil moisture and soil temperature.

56 This simple model structure has recently received some criticism because its lack explicit
57 representation of microbial physiology (Allison et al., 2010; Todd-Brown et al., 2012; Wieder
58 et al., 2013; Xenakis and Williams, 2014). Furthermore, the formulation of the environmental
59 scalar is held constant in time which is not consistent with recently identified enhancing or
60 compensatory responses of microbial communities to changes in boundary conditions (Karhu

61 et al., 2014). Therefore, it can only explain the acclimation of decomposers to warming (Luo
62 et al., 2001) as a result of the quick depletion of labile pools by enhanced microbial biomass
63 (Kirschbaum, 2004; Knorr et al., 2005).

64 We previously identified (Exbrayat et al., 2013b, 2014) some further implications of the first-
65 order representation of microbial decomposition. First, in climate change experiments, model
66 pools are usually initialised using a spin-up procedure with fixed pre-industrial atmospheric
67 CO₂ concentrations until C pool trends are removed (Xia et al., 2012). Due to the interaction
68 with substrate availability, the decay rate simulated by the model in response to steady
69 boundary conditions determines the size of soil C pools reached at equilibrium. Because spin-
70 up is a long computational process, the magnitude of pool sizes is conserved during
71 subsequent shorter simulations of climate change and, as a result, equilibrated stocks strongly
72 explain final stocks (e.g. CMIP5 models as shown in supplementary Figure S1 after Exbrayat
73 et al., 2014). Second, the microbial sensitivity to changing environmental conditions affects
74 the response of the system under transient climate simulations (Falloon et al., 2011; Exbrayat
75 et al., 2013a,b). However, because substrate availability also controls the amount of respired
76 carbon, there is a “memory” control imposed by the initial conditions of this transient
77 simulation (Exbrayat et al., 2013b and 2014) that also affects the response to perturbation in
78 boundary conditions. The relative contribution of these two factors on soil C projections
79 remains to be explored in detail especially since last generation models disagree on the
80 carbon balance projected in the future (Friedlingstein et al., 2014; Nishina et al., 2014),
81 making it challenging to elaborate any land-based offsetting strategy.

82 Here, we use a reduced complexity model representative of current state-of-the-art models of
83 soil organic C decomposition. A systematic sensitivity analysis is performed to disentangle
84 the effect of the time-invariant baseline residence time and the formulation of the dynamic
85 response of microbial decomposition to climatic change on soil C dynamics at regional and
86 global scale. Using these experiments, we seek to investigate the relative contribution of
87 these two inter-related components that drive the absolute and relative change in soil C
88 through time. This is a step towards understanding the origin of the disagreement between
89 CMIP5 models’ simulation of soil C and can help in reducing the uncertainty in future model
90 intercomparisons. We also use available estimates of total soil C to assess the added value of
91 observational data to inform the modelling procedure. We attempt to constrain the system’s
92 response to climate change by identifying model versions that simulate amounts of soil C

93 mobilized in the active cycle that are outside the confidence intervals estimated for the
 94 observations. We argue that, due to the first-order parameterization, such model versions are
 95 unlikely to provide reliable projections of the response of soil C pools as they would do it for
 96 the wrong reasons. We do not aim to provide new estimates of SOC response to climate
 97 change with our reduced complexity model. Instead, we suggest that our results will help the
 98 CMIP6 community to improve the design of future intercomparisons by highlighting the need
 99 and benefits of confronting models with existing data to reduce the uncertainty.

100

101 **2 Materials and methods**

102 **2.1 Reduced complexity model**

103 It is not possible to re-run each CMIP5 model or isolate the representation of soil carbon
 104 processes from each model. This would be extraordinarily computationally expensive and the
 105 associated feedbacks would make the analysis of the results problematic. A far simpler
 106 approach is required which led Todd-Brown et al., (2013, 2014) to develop and demonstrate
 107 that the CMIP5 SOC dynamics can be successfully reproduced using a simplified model
 108 structure. In this paper we develop and then use a reduced complexity model that simulates
 109 the monthly evolution of a single soil organic carbon pool, C_s , in response to input derived
 110 from Net Primary Productivity (NPP , $\text{g C m}^{-2} \text{ mth}^{-1}$) and output by heterotrophic respiration
 111 (R_h , $\text{g C m}^{-2} \text{ mth}^{-1}$). For each monthly time step, the soil carbon balance can be described as:

$$112 \quad \frac{\partial C_s}{\partial t} = NPP - R_h \quad (1)$$

113 where NPP is a prescribed boundary condition in our model and R_h is simulated as a first-
 114 order process dependent on the availability of substrate C_s such as:

$$115 \quad R_h = k^{-1} \cdot f_T \cdot f_W \cdot C_s \quad (2)$$

116 where k is the baseline residence time at 15°C (Xia et al., 2013) adjusted at each time step by
 117 f_T which is a function of soil temperature T_s ($^\circ\text{C}$). The soil moisture (θ_s) modification
 118 function, f_W , is usually expressed as a fraction of soil moisture saturation (Moyano et al.,
 119 2012). We implement a classical formulation of the soil temperature sensitivity function f_T :

$$120 \quad f_T = Q_{10}^{\frac{(T_s - T_{ref})}{10}} \quad (3)$$

121 where Q_{10} is a constant factor that describes the relative increase in microbial activity for a
 122 warming of 10°C, and T_{ref} is the reference temperature (°C) for which $f_T(T_s) = 1$ (Lloyd and
 123 Taylor, 1994; Bauer et al., 2012). The chosen T_{ref} is the commonly used 15°C (Todd-Brown
 124 et al., 2013) so that the decomposition rate equals k^{-1} when moisture is non-limiting and
 125 temperature is approximately equal to the global average. We use the same formulation of f_W
 126 as in the CASA-CNP model (Wang et al., 2010):

127  (4)

128 which is a bell-shaped function that is equal to 1 for $\theta_s = 0.55$.

129 This first-order representation of microbial decomposition with a specified decay rate
 130 adjusted by environmental scalars is used in all 11 CMIP5 models that simulate soil carbon
 131 (Todd-Brown et al., 2013) and all 7 Dynamic Global Vegetation Models used in the ISI-MIP
 132 project (Friend et al., 2013; Nishina et al., 2014). Typically, these models rely on a multi-pool
 133 architecture to represent the diversity in organic matter. Each pool has its own residence time
 134 that corresponds to a degree of resistance to decomposition (Davidson and Janssen, 2006).
 135 Usually, part of the decomposition occurring in one pool is routed to one or several other
 136 pools while the rest is emitted via R_h . At the ecosystem scale, however, the same
 137 environmental scalar is applied despite the multi-pool architecture, and the heterotrophic
 138 respiration flux is proportional to the amount of substrate available. Therefore, our simplified
 139 model is broadly representative of the current paradigm and provides a useful framework to
 140 undertake the sensitivity analysis described hereafter.

141 Soil moisture also has an influence on microbial decomposition (Falloon et al., 2011, Moyano
 142 et al., 2012, 2013; Exbrayat et al., 2013a,b). However, Todd-Brown et al. (2013, 2014)
 143 recently demonstrated that a one pool reduced complexity model could reproduce both total
 144 soil carbon content and its spatial distribution for most of the CMIP5 models without
 145 considering decomposition response to variations in soil moisture. We also recently showed
 146 that global features in the distribution and evolution of C_s were much more related to
 147 uncertainties in f_T than uncertainties in the formulation of f_W (Exbrayat et al., 2013b).
 148 Therefore, in order to keep the analyses as simple as possible and isolate the effect of f_T but
 149 still account for the effect of soil moisture on R_h , we keep the formulation of f_W constant in
 150 the experiments that follow.

151 We are aware that our reduced complexity model relies on simplifications such as the use of a
152 single soil carbon pool and global values of k , Q_{10} and T_{ref} . While we agree that a multiple
153 pool structure would provide diverging results, single pool soil carbon carbon models similar
154 to our design are used in 3 of the 11 CMIP5 models described by Todd-Brown et al. (2013)
155 and 2 of the 7 ISI-MIP models described by Nishina et al. (2014). Further, using global
156 parameter values of k , Q_{10} and T_{ref} is consistent with these state-of-the-art models (Todd-
157 Brown et al., 2013; Nishina et al., 2014). Of course, this does not allow representing
158 processes such as the remobilization of carbon in the active cycle following permafrost thaw
159 (Koven et al., 2011) or the probably different behaviour of biological systems in frozen
160 conditions but these are not implemented in the land component of CMIP5 Earth system
161 models and therefore fall beyond the scope of this paper. In summary, we fully appreciate
162 that our reduced complexity model is a simplification of the processes that operate in various
163 regions of the Earth System. However, we note that our study investigates the sensitivity of
164 the first-order parameterization of microbial decomposition and R_h processes used in *current*
165 *ecosystem models* to its uncertain parameters (Todd-Brown et al., 2013; Nishina et al., 2014).
166 Our approach is therefore analysing how current models behave and why current models
167 simulate a large range in SOC. Our purpose is not to provide improved results of the response
168 of soil carbon to climate change but rather to better understand the implications of existing
169 approaches, using in CMIP5, to parameterization and initial value prescription described in
170 Section 2.2.

171 **2.2 Model setup and experiments**

172 We configure the reduced complexity model in a spatially explicit way to represent global
173 variations, implemented as a surrogate for the CASA-CNP biogeochemical module (Wang et
174 al., 2010) of the CABLE land surface model (Wang et al., 2011). A previous simulation by
175 CABLE coupled to the coarse-resolution CSIRO Mk3L climate model (3.2° latitude \times 5.6°
176 longitude; Phipps et al., 2011) and driven by CMIP5 atmospheric CO_2 data provides monthly
177 NPP , T_s and θ_s to the reduced complexity model. We use both historical simulations
178 (Exbrayat et al., 2013b) and 21st century projections using the Representative Concentration
179 Pathway 8.5 (RCP 8.5) atmospheric concentration scenario.

180 We perform a sensitivity analysis by running the simple model with various combinations of
181 a Q_{10} value and a baseline residence time k . We use 11 equally-spaced values of Q_{10} ranging

182 from 1.5 to 2.5 (i.e. intervals of 0.1), and 31 equally-spaced values of k ranging from 120
183 months to 480 months (i.e. intervals of 12 months). These values are based on the range of
184 results previously obtained by Todd-Brown et al. (2013) with their own reduced complexity
185 model. Each value of Q_{10} is applied with each value of k for a total of 341 simulations. Model
186 versions are initialised via a classical spin-up procedure (Xia et al., 2012) using input data
187 from 1850 to 1859 for 10,000 years to ensure all soil carbon pools reach a steady-state. We
188 then continue simulations with NPP , T_s and θ_s data from 1850 to 2005, and continue with
189 RCP 8.5 projections to 2100. We note that these drivers do not include the representation of
190 land-use and land cover change and their effect on NPP , T_s and θ_s . Therefore, SOC input are
191 likely to be higher than in reality. However, as stated earlier we are using the reduced
192 complexity framework to understand the behaviour of the SOC model in response to
193 variations in its parameters and we do not aim to provide improved estimates of global scale
194 terrestrial carbon sinks. In each model version, both k and the sensitivity of R_h to temperature
195 (represented by Q_{10}) are constant globally, in accordance with observations (Mahecha et al.,
196 2010) and state-of-the-art models (Todd-Brown et al., 2013; Nishina et al., 2014). However,
197 the actual value of the environmental scalar f_T will of course vary spatially and temporally as
198 a function of T_s . As we keep the same formulation of f_W between model versions, we can
199 attribute differences in results to the values of Q_{10} or k .

200

201 **2.3 Harmonized World Soil Database**

202 The Harmonized World Soil Database (HWSD; FAO, 2012) combines several national
203 inventories and provides a number of chemical and physical soil properties at a 30 arc second
204 resolution globally. However, despite the availability of this dataset, CMIP5 models exhibit a
205 six-fold range in their total soil carbon content (Todd-Brown et al., 2013) including values
206 well outside the uncertainty boundaries of observational data. We previously showed that
207 simply using the global amount of SOC from the HWSD dataset to discriminate between
208 acceptable and unacceptable simulations resulted in a non-negligible reduction of the
209 uncertainty in historical net carbon uptake (Exbrayat et al., 2013b). While we do not aim to
210 provide CMIP5-like projections of the soil carbon balance with our reduced complexity
211 model, we investigate the value of using the HWSD to discriminate between plausible and
212 implausible simulations.

213 We follow the method described by Todd-Brown et al. (2013) to derive an estimate of current
214 total soil carbon from the latest version of the Harmonized World Soil Database (HWSD).
215 First, we re-grid the original 30 arc seconds raster to a $0.5^\circ \times 0.5^\circ$ resolution. Within each
216 half-degree cell we select the dominant soil type. For each soil type, the database provides
217 bulk density and organic carbon content for a top layer (0 – 30 cm depth) and a bottom layer
218 (30 – 100 cm depth). This allows us to calculate soil C density (in kg C m^{-2}) in each cell. We
219 then multiply each grid cell by its area and sum to obtain a global estimate of ~ 1170 Pg C.
220 Similarly to Todd-Brown et al. (2013) we also consider the uncertainty associated to our re-
221 gridding process as well as analytical measurements of soil properties. We therefore obtain a
222 95% confidence interval (CI_{95}) of 29% below the mean to 32% above the mean, or $\sim 830 -$
223 1550 Pg C. We provide these gridded data as supplementary material. Due to the 6-fold range
224 of SOC simulated by CMIP5 models (Todd-Brown et al., 2013), we believe that global SOC
225 stocks from the HWSD can already represent a strong constraint to discriminate between
226 different simulations.

227

228 **3 Results**

229 **3.1 Total soil carbon and global balance**

230 Figure 1 presents snapshots of total soil carbon for all 341 model versions for three periods:
231 at equilibrium (in 1850, Figure 1a), at the end of historical transient simulations (in 2005,
232 Figure 1b), and at the end of the projections with forcing corresponding to RCP 8.5 (in 2100,
233 Figure 1c). Figure 1a shows that the spin-up procedure causes different model versions to
234 equilibrate at widely varying levels of total soil carbon despite the use of the same boundary
235 conditions of NPP and T_s . Differences in residence time k contribute most of the ~ 592 to
236 2745 Pg C range, with larger values of k resulting in larger pools (Figure 1a). Variations in
237 the Q_{10} parameter of f_T have a smaller influence on total soil carbon but lower values do result
238 in lower total soil carbon. For the same value of k , simulations with $Q_{10} = 1.5$ equilibrate with
239 total soil carbon equal to $86\% \pm 0.005\%$ (mean ± 1 standard deviation) of the amount with
240 $Q_{10} = 2.5$. Figure 1b shows that the distribution of total soil carbon between model versions
241 does not vary much during historical simulations (1850-2005). Models with large total soil
242 carbon pools over this period remain versions with long residence time k and higher values of
243 Q_{10} . Note, however, that the range of total soil carbon in 2005 grows to ~ 709 to 2943 Pg C.

244 Dashed contours on Figure 1b indicate the limits of the CI_{95} of the HWSD for current total
245 soil carbon. Here, 115 simulations with values of k ranging approximately from 150 to 250
246 months all fall within this range for 2005, regardless of the Q_{10} value used. Finally, Figure 1c
247 continues to indicate a strong control of k on the total soil carbon in 2100. The projected
248 range narrows to ~684 to 2825 Pg C throughout the 21st century. However, we note there is
249 an inversion in the influence of Q_{10} on simulated total soil carbon with lower values of Q_{10}
250 resulting in larger pools especially for longer baseline residence times k . Nevertheless, this is
251 still minor compared to the influence of k on C_s .

252 Although the range in simulated soil carbon remains similar through time, non-negligible
253 changes occur. This is highlighted in Figure 2 which shows ΔC_s , the change in total soil
254 carbon as a function of model parameters k and Q_{10} for the historical simulations (1850 –
255 2005, Figure 2a) and RCP 8.5 projections (2006 – 2100, Figure 2b). First, Figure 2a clearly
256 shows that all model versions act as a net carbon sink during historical simulations,
257 accumulating between 81 and 283 Pg C. Model versions with longer residence time k tend to
258 accumulate more carbon through time. However, models with the largest value of Q_{10} tend to
259 accumulate only $69\% \pm 0.4\%$ (mean ± 1 standard deviation) of the amount that the lowest Q_{10}
260 models do. By analysing Figure 2b, we see that the influence of Q_{10} on the total soil carbon
261 balance grows during RCP 8.5 projections where Q_{10} now determines whether the soil
262 remains a sink or becomes a source. This change between a source or a sink for different Q_{10}
263 values follows a near linear relationship with k (solid line on Figure 2b). Interestingly, the -
264 179 to 168 Pg C range in the change in total soil carbon during RCP 8.5 is mostly a function
265 of Q_{10} as both extremes are achieved with the longest residence time used here. In other
266 words, while Q_{10} decides of the sign of the change, k , and hence the initial stocks of SOC
267 after spin-up, drives the magnitude of the response.

268 If we consider only models that fall within the CI_{95} of the HWSD for current total soil carbon
269 (dashed contours on Figure 2a and 2b) the spread in simulated total soil carbon balance is
270 largely reduced. During the historical simulations, the range of this subset of models shrinks
271 by 84 Pg C to between 87 and 205 Pg C. It corresponds to a reduction of about 42% of the
272 initial uncertainty. Similarly, the range in projected soil carbon balance is reduced by 157 Pg
273 C to -129 to 61 Pg C, a reduction of about 45% of the initial uncertainty. We note, however,
274 that this restriction does not necessarily increase confidence in sign of the future soil carbon
275 change under RCP8.5.

276 Differences in the behaviour between the full set of models and this subset of observationally
277 constrained models can be seen in the time series and probability density functions (PDFs)
278 for the historical period, shown in Figure 3. First, the time series from 1850 shows there is no
279 noticeable difference between the full set of simulations (in grey) and the subset of
280 simulations with acceptable current soil carbon (in green) until 1900. During the first half of
281 the 20th century, stronger sinks are excluded as they lie outside the CI₉₅ range, which
282 correspond to the upper tail of the distribution of ΔC_s (see PDF inset for 1950). However, the
283 kurtosis of the distribution, or most probable change from our simulations, changes
284 negligibly. After ~1960, we observe a step-change in cumulative ΔC_s that follows a strong
285 response in NPP to the rapid increase in atmospheric CO₂ (please refer to Exbrayat et al.,
286 2013b for a more detailed account of this behaviour). The spread between simulations grows
287 and most of the excluded simulations based on the CI₉₅ range are the strongest sinks (as in
288 Figure 2a) while a few of the least accumulating simulations are also excluded. This does
289 have a large impact on the most probable change in storage, reducing it from ~200 PgC to
290 ~140 PgC.

291 We now examine future simulations and present time series and PDFs of change in total soil
292 carbon during RCP 8.5 projections in Figure 4. All simulations continue to accumulate
293 carbon at the beginning of the 21st century and remain net carbon sinks until about 2060. At
294 the end of the century, some model versions have simulated positive ΔC_s corresponding to a
295 net carbon sink over the 21st century, while other ends their projections with negative ΔC_s , or
296 a net carbon loss. However, all simulations show the same overall behaviour with first an
297 increase in C_s that peaks, and then a decrease in C_s . The timing of the peak, i.e. when soil
298 carbon starts to deplete, varies between ~2035 and 2075 and is explained by the value of Q_{10}
299 ($R^2 = 0.74$, data not shown) with higher values leading to an earlier peak. This indicates that,
300 in all simulations, soil has become a net source of carbon by the end of the 21st century,
301 regardless how much carbon was accumulated since 2005, and hence since 1850. The PDFs
302 in 2050 show that selecting only observationally consistent models results in the most heavily
303 accumulating simulations, i.e. those that would peak later, to be dismissed. However, by
304 2100, both the lower and upper tails of the initial distribution are clipped, reducing the
305 simulated range from -178 to 168 Pg C (all simulations) to -129 to 61 Pg C. In both cases,
306 differences in the kurtosis of both distributions remains very small which indicates that our

307 selection scheme dismisses outliers. We note that the lower bound of ΔC_s for both sets of
308 models is the same until late in the projections (~2085).

309

310 **3.2 Regional differences**

311 Although Figure 1 indicates that the range in k can explain most of the variability in total soil
312 carbon content at equilibrium and hence through transient simulations, Q_{10} is likely to
313 influence the local response of f_T . Figure 5 shows the relative value of f_T for different
314 temperatures and values of Q_{10} . Since the chosen $T_{ref}=15^\circ\text{C}$, all Q_{10} values lead f_T to be equal
315 at this particular temperature. However, the more difference there is between the actual
316 temperature and T_{ref} , the more sensitive f_T becomes to values of Q_{10} . As our simulations are
317 spatially-explicit, this may introduce non-negligible regional differences in C pools at
318 equilibrium and their response to transient changes in T_s and NPP.

319 To investigate this more in detail, we present the zonal averages of soil C density for different
320 values of Q_{10} with k set to 180 months (Figure 6). We choose this particular residence time as
321 example because all corresponding simulations are within the CI₉₅ of the HWSD for 2005
322 regardless the value of Q_{10} . Figure 6a shows that Q_{10} values do introduce non-negligible
323 differences in local equilibrated soil C density. Steady-state pools at low latitudes (30°S to
324 30°N) are larger with low values of Q_{10} (blue in Figure 6). Conversely, high latitude pools are
325 larger with high values of Q_{10} (red in Figure 6). Overall, the range in the value of zonally
326 averaged soil C density at equilibrium is up to three-fold depending on the chosen value of
327 Q_{10} . This is particularly obvious in regions with high NPP including low-latitude tropical
328 rainforests or northern taigas. As was the case with total C_s , the zonal distribution soil C
329 density and the relative position of simulations with different Q_{10} do not vary much between
330 1850 and 2005 (Figure 6b) although there is a slight shift towards uniformly higher densities
331 as all model versions are net global carbon sinks (Figure 2a and 3). The pattern of zonal soil
332 carbon remains essentially the same at the end of RCP 8.5 projections. However, models with
333 lower values of Q_{10} now have more carbon than those with high values of Q_{10} over a broader
334 zone (40°S – 50°N).

335 Figure 7 shows the zonal change in soil C density for the same simulations as in Figure 6.
336 Figure 7a indicates that all simulations simulate a net sink almost everywhere during
337 historical simulations, except at latitudes $> 70^\circ\text{N}$. However, the strength of this sink is

338 strongly dependent upon the value of Q_{10} , especially in low latitudes. There is an
339 approximately two-fold difference between the high accumulation of low Q_{10} models, and the
340 low accumulation of high Q_{10} models. Differences between Q_{10} values are negligible at
341 higher latitudes. Figure 7b shows the same information for RCP 8.5 projections. Simulations
342 with lower values of Q_{10} almost always accumulate more C (except between 0° and 10°N).
343 While all model versions with $k = 180$ months lose carbon at low latitudes ($20^\circ\text{S} - 20^\circ\text{N}$),
344 and gain carbon at high latitudes in the northern hemisphere ($> 50^\circ\text{N}$), the value of Q_{10} , and
345 hence the environmental scalar f_T , decides of the sign of the local soil C balance in the 21st
346 century at mid-latitudes. Within the mid-latitudes, high values of Q_{10} are more likely to
347 simulate a net loss of soil carbon. We can therefore narrow down the dependence of the
348 global ΔC_s on Q_{10} to its affect at mid-latitudes.

349

350 **4 Discussion**

351 **4.1 Effect of k and Q_{10} on soil carbon**

352 In our simulations, the range in total soil carbon at equilibrium (~ 592 to 2745 Pg C) depends
353 on which value of Q_{10} and especially k is used (Figure 1a). This range captures the ~ 561 to
354 2938 Pg C range in soil carbon in CMIP-5 in 1860 (see Supplementary Figure S1). We note
355 of course that CMIP5 models not only vary in their soil C component, but simulate different
356 NPP and T_s and also integrate a range of soil moisture limitations (Todd-Brown et al., 2013).
357 The range achieved here at the end of the historical simulations (~ 709 to 2943 Pg C) is, for
358 example, larger than the 1090 to 2646 Pg C range in 2000 from 7 DGVMs in the ISI-MIP
359 project (Nishina et al., 2014) which were driven by a harmonised weather dataset.

360 We can attribute this range to the first-order representation of decomposition and its response
361 to the initialisation procedure used in most CMIP-5 simulations. By spinning-up the model,
362 the goal is to stabilise pools so that total NPP is exactly compensated by total R_h over the
363 selected period of time (here 10 years). In Equation (2), a longer residence time k results in a
364 lower decay rate (i.e. R_h per unit of C_s). Therefore, model versions that have a slower
365 turnover will require more substrate to simulate the same R_h needed to compensate NPP . As
366 the baseline residence time k is applied globally, it drives the global pool size (Figure 1)
367 much more than changing Q_{10} affects f_T . However, as seen in Figure 6, when considered
368 regionally, Q_{10} plays a non-negligible role for the local response of decomposition and the

369 definition of equilibrium soil C density. High values of Q_{10} lead f_T to trigger strong decay
370 rates in warm regions (Figure 5) that require less substrate (see low latitudes in Figure 6a) to
371 compensate the same NPP . Conversely, high Q_{10} lead to low values of f_T in cold regions.
372 Therefore, more substrate is required to bring the pool to equilibrium as seen in high latitudes
373 in Figure 6a. Low values of Q_{10} show an opposite regional behaviour. Regional differences
374 compensate each other and therefore f_T with different Q_{10} values can only explain a small
375 fraction of the range in equilibrated total soil carbon. Of course, if another T_{ref} was used, the
376 relative differences between f_T with different Q_{10} would be altered and the influence of Q_{10}
377 and its effect on f_T on total and local C_s would vary. Furthermore, the difference between f_T
378 with different Q_{10} grows with the absolute value of the difference $T_s - T_{ref}$. Therefore, using a
379 value of T_{ref} that is outside the range of actual temperatures would lead f_T with different Q_{10} to
380 keep the same relative position globally. It would introduce larger relative differences
381 between these functions.

382 Comparing Figures 1a, 1b and 1c suggests that the range in total C_s at equilibrium is a good
383 predictor of the current and future range in total soil carbon. Despite differences in the
384 magnitude of the change in C_s through time (Friedlingstein et al., 2014), equilibrium
385 conditions achieved under pre-industrial conditions largely define current and future pool
386 sizes as observed in CMIP5 models (Exbrayat et al., 2014). Examining Figure 6 confirms that
387 this global effect can also be seen regionally, especially in low (20°S to 20°N) and high
388 (>50°N) latitudes, where carbon pools are largest. This is of concern as substrate availability
389 also influences R_h and hence its response to changes.

390 Changes in C_s through time are nevertheless non-negligible, and it is important to quantify
391 the response of the system to perturbations. Our results show increasing atmospheric CO_2
392 concentrations enhances NPP more than the simultaneous warming enhances R_h during
393 historical simulations. This historical net carbon sink that is driven by the response of
394 vegetation to increasing atmospheric CO_2 (and hence SOC_{in}) is in accordance with previous
395 studies (Friedlingstein et al., 2006; Sarmiento et al., 2010; Zhang et al., 2011; Wania et al.,
396 2012; Anav et al., 2013; Exbrayat et al., 2013b). Therefore, all model versions with longer
397 residence time accumulate more C_s over the same time period as a result of a slower turnover
398 of carbon in soils, and this mirrors the state of the equilibrium stores. However, despite the
399 dominance of the increased NPP on ΔC_s , the historical warming signal is influential.
400 Specifically, those model versions more sensitive to changes in temperature (i.e. with high

401 values of Q_{10}) accumulate less soil carbon during the 20th century even though they initially
402 equilibrated with larger global pools. This is also true of local soil C density where high Q_{10}
403 values are less accumulating regardless of the initial soil C density. We however note that the
404 value T_{ref} used in our experiments is well within the range of actual temperatures. Therefore,
405 the historical warming does not induce large changes in the values of f_T with different Q_{10} .

406 Projections under the strong-forcing RCP 8.5 scenario also see an increase in the influence of
407 the value of Q_{10} on ΔC_s . Figure 2b clearly shows that the capacity of soils to become carbon
408 sources or remain sinks depends almost entirely on the Q_{10} parameter, and both states can be
409 achieved for any value of k used while remaining within range of previous studies
410 (Friedlingstein et al., 2014; Nishina et al., 2014). Figure 7b indicates that this is clearly a
411 result of differences in the local response of model versions in the mid-latitudes as a function
412 of Q_{10} . Such regional discrepancies leading to a change in the sign of global ΔC_s models have
413 also been highlighted through a recent inter-comparison project that used a harmonised
414 weather dataset to drive 7 biome models (Nishina et al., 2014). However, contrary to this
415 previous study, none of our model versions accumulates soil carbon in the inter-tropical
416 region during the 21st century. This is probably due to the fact that we use the same boundary
417 conditions of NPP and T_s for all our model versions, while models used by Nishina et al.
418 (2013) used a prescribed weather dataset but were left free to simulate their own NPP .

419 Overall, the globally applied model parameter k drives the steady-state response of our
420 reduced complexity system. However, the more conditions are changing (i.e. steady-state to
421 historical to RCP 8.5 projections), the more the dynamic transition of the system towards a
422 new equilibrium depends on the environmental scalar f_T and the specific value of Q_{10} .
423 Although the same formulation of f_T is applied globally, differences in its response to local T_s
424 sum up to determine the sign of total soil carbon balance. We also note that model versions
425 that equilibrate as a result of longer baseline residence time k have a tendency to produce a
426 larger absolute response of total soil carbon balance. Therefore, the size of pools to which the
427 change is applied seems to dominate the response even when higher values of k imply a
428 smaller relative change in the decay rate $k^{-1} \times f_T \times f_W$ used in equation 2. This control of
429 initial conditions obtained by spin-up on the response of the system is a critical aspect that
430 needs to be better resolved, especially since recent inter-comparison experiments all exhibit
431 huge discrepancies in equilibrium conditions of participating models (Anav et al., 2013;
432 Todd-Brown et al., 2013; Nishina et al., 2014).

434 **4.2 Discriminating between model versions**

435 Since k clearly influences the total soil carbon content at equilibrium in 1850, it is a good
436 predictor of the current total soil carbon content. Therefore, k is the key parameter that
437 decides how much carbon is active in the modelled system, and whether model versions fall
438 within the CI₉₅ of the HWSD. Here, all simulations with baseline residence time between 150
439 and 250 months fulfil this requirement regardless of which Q_{10} is used in f_T .

440 If we isolate these simulations, the range in total soil carbon change shrinks by 42% and 45%
441 for the historical simulations and RCP 8.5 projections, respectively. However, while this
442 selection dismisses outliers it does not increase confidence in the sign of the soil carbon
443 change. This is because regional differences lead to similar values in total soil carbon for
444 different values of Q_{10} . These regional differences translate into heterogeneous responses
445 under RCP 8.5 forcing, especially in mid-latitudes. They are sufficient to induce a change of
446 sign in the global soil carbon balance.

447

448 **5 Conclusion**

449 We have used a reduced complexity model, broadly representative of current state-of-the-art
450 models of soil organic C decomposition used in CMIP5 and ISI-MIP experiments, to explore
451 the response of microbial decomposition to climate change on soil C dynamics at regional
452 and global scale. We have shown that key parameters in the first-order representation of
453 decomposition interact in markedly different ways depending on the nature of forcing and
454 antecedent conditions. First, the time and space-invariant baseline residence time decides of
455 the total soil carbon content at equilibrium after spin-up, typically the process used by CMIP5
456 models to initialise C pools. Next, the more boundary conditions imposed on the system
457 move away from the equilibrium forcing, the more the environmental scalar describing the
458 sensitivity of the system gains in importance. However, it is the size of the pool to which the
459 change is applied that mostly controls the magnitude of the response.

460 Applying a constraint on total soil carbon that discriminates between acceptable simulations -
461 of total soil carbon leads to a drastic reduction of the range of simulated change. Meanwhile,
462 most of the remaining uncertainty in 21st century projections of total soil carbon can be

463 attributed to zonal differences in the response to change, especially at mid-latitudes. These do
464 not allow us to confidently project soil as either a global source or sink of carbon for the 21st
465 century. However, it is clear that under RCP 8.5 tropical soils are not suited for long-term
466 carbon storage while some more potential exists in high latitudes.

467 Finally, we suggest that future estimates of terrestrial, and especially soil, carbon responses to
468 climate change should be more constrained by available datasets of carbon stocks. This is
469 critical as model structures describe fluxes as a fraction of the substrate pool size. So far, the
470 process of spin-up has too many degrees of freedom that lead to model-specific amounts of
471 active soil carbon.

472

473 **Acknowledgements**

474 This work was supported by the Australian Research Council ARC grant DP110102618 and
475 the ARC Centre of Excellence for Climate System Science grant CE110001028. CSIRO
476 Mk3L model runs were made possible by the NCI National Facility at the Australian National
477 University via the provision of computing resources to the ARC Centre of Excellence for
478 Climate System Science. We thank Dr. K. E. O. Todd-Brown for guidance in processing the
479 HWSD dataset.

480

481 **References**

482 Ahlström, A., Smith, B., Lindström, J., Rummukainen, M., and Uvo, C. B.: GCM
483 characteristics explain the majority of uncertainty in projected 21st century terrestrial
484 ecosystem carbon balance, *Biogeosciences*, 10, 1517-1528, doi:10.5194/bg-10-1517-2013,
485 2013.

486 Allison, S. D., Wallenstein, M. D. and Bradford, M. A.: Soil-carbon response to warming
487 dependent on microbial physiology, *Nat. Geosci.*, 3(5), 336–340, doi:10.1038/ngeo846, 2010.

488 Anav, A., Friedlingstein, P., Kidston, M., Bopp, L., Ciais, P., Cox, P., Jones, C., Jung, M.,
489 Myneni, R., and Zhu, Z.: Evaluating the land and ocean components of the global carbon
490 cycle in the CMIP5 Earth systems models, *J. Clim.*, 26, 6801–6843, doi:10.1175/JCLI-D-12-
491 00417.1, 2013.

492 Bauer, J., Weihermüller, L., Huisman, J., Herbst, M., Graf, A., Séquaris, J. and Vereecken,
493 H.: Inverse determination of heterotrophic soil respiration response to temperature and water
494 content under field conditions, *Biogeochemistry*, 108(1), 119–134, doi:10.1007/s10533-011-
495 9583-1, 2012.

496 Davidson, E. A. and Janssens, I. A.: Temperature sensitivity of soil carbon decomposition
497 and feedbacks to climate change, *Nature*, 440(7081), 165–173, doi:10.1038/nature04514,
498 2006.

499 Exbrayat, J.-F., Pitman, A. J., Abramowitz, G. and Wang, Y.-P.: Sensitivity of net ecosystem
500 exchange and heterotrophic respiration to parameterization uncertainty, *J. Geophys. Res.*
501 *Atmospheres*, 118(4), 1640–1651, doi:10.1029/2012JD018122, 2013a.

502 Exbrayat, J.-F., Pitman, A. J., Zhang, Q., Abramowitz, G., and Wang, Y.-P.: Examining soil
503 carbon uncertainty in a global model: response of microbial decomposition to temperature,
504 moisture and nutrient limitation, *Biogeosciences*, 10, 7095-7108, doi:10.5194/bg-10-7095-
505 2013, 2013b.

506 Exbrayat, J.-F., Pitman, A. J., and Abramowitz, G.: Response of microbial decomposition to
507 spin-up explains CMIP5 soil carbon range until 2100, *Geosci. Model Dev. Discuss.*, 7, 3481-
508 3504, doi:10.5194/gmdd-7-3481-2014, 2014.

509 Falloon, P. D., Jones, C. D., Ades, M. and Paul, K.: Direct soil moisture controls of future
510 global soil carbon changes: An important source of uncertainty, *Glob. Biogeochem. Cycles*,
511 25, GB3010, doi: 10.1029/2010GB003938, 2011.

512 FAO/IIASA/ISRIC/ISSCAS/JRC: Harmonized World Soil Database (version 1.21), FAO,
513 Rome, Italy and IIASA, Laxenburg, Austria, 2012.

514 Friedlingstein, P., Cox, P., Betts, R., Bopp, L., von Bloh, W., Brovkin, V., Cadule, P., Doney,
515 S., Eby, M., Fung, I., Bala, G., John, J., Jones, C., Joos, F., Kato, T., Kawamiya, M., Knorr,
516 W., Lindsay, K., Matthews, H. D., Raddatz, T., Rayner, P., Reick, C., Roeckner, E.,
517 Schnitzler, K.-G., Schnur, R., Strassmann, K., Weaver, A. J., Yoshikawa, C. and Zeng, N.:
518 Climate–Carbon Cycle Feedback Analysis: Results from the C⁴MIP Model Intercomparison,
519 *J. Clim.*, 19, 3337–3353, doi:10.1175/JCLI3800.1, 2006.

520 Friedlingstein, P., Meinhausen, M., Arora, V. K., Jones, C. D., Anav, A., Liddicoat, S. K.,
521 and Knutti, R.: Uncertainties in CMIP5 climate projections due to carbon cycle feedbacks, *J.*
522 *Clim.*, 27, 511-526, doi:10.1175/JCLI-D-12-00579.1, 2014.

523 Friend, A. D., et al: Carbon residence time dominates uncertainty in terrestrial vegetation
524 responses to future climate and atmospheric CO₂, *Proc. Natl. Acad. Sci.*, in press, 2013.

525 Kahru, K., Auffret, M. D., Dungait, J. A. J., Hopkins, D. W., Prosser, J. I., Singh, B. K.,
526 Subke, J.-A., Wookey, P. A., Ågren, G. I., Sebastià, M.-T., Gouriveau, F., Bergkvist, G.,
527 Meir, P., Nottingham, A. T., Salinas, N. and Hartley, I. P.: Temperature sensitivity of soil
528 respiration rates enhanced by microbial community response, *Nature*, 513, 81-84,
529 doi:10.1038/nature13604, 2014.

530 Kirschbaum, M. U. F.: Soil respiration under prolonged soil warming: are rate reductions
531 caused by acclimation or substrate loss?, *Glob. Change Biol.*, 10(11), 1870–1877,
532 doi:10.1111/j.1365-2486.2004.00852.x, 2004.

533 Knorr, W., Prentice, I. C., House, J. I. and Holland, E. A.: Long-term sensitivity of soil
534 carbon turnover to warming, *Nature*, 433(7023), 298–301, doi:10.1038/nature03226, 2005.

535 Koven, C. D., Ringeval, B., Friedlingstein, P., Ciais, P., Cadule, P., Khvorostyanov, D.,
536 Krinner, G. and Tarnocai, C.: Permafrost carbon-climate feedbacks accelerate global
537 warming, *Proc. Natl. Acad. Sci.*, 108(36), 14769–14774, doi:10.1073/pnas.1103910108,
538 2011.

539 Lloyd, J. and Taylor, J. A.: On the Temperature Dependence of Soil Respiration, *Funct.*
540 *Ecol.*, 8(3), 315–323, doi:10.2307/2389824, 1994.

541 Luo, Y., Wan, S., Hui, D. and Wallace, L. L.: Acclimatization of soil respiration to warming
542 in a tall grass prairie, *Nature*, 413(6856), 622–625, doi:10.1038/35098065, 2001.

543 Mahecha, M. D., Reichstein, M., Carvalhais, N., Lasslop, G., Lange, H., Seneviratne, S. I.,
544 Vargas, R., Ammann, C., Arain, M. A., Cescatti, A., Janssens, I. A., Migliavacca, M.,
545 Montagnani, L. and Richardson, A. D.: Global Convergence in the Temperature Sensitivity
546 of Respiration at Ecosystem Level, *Science*, 329(5993), 838–840,
547 doi:10.1126/science.1189587, 2010.

548 Nishina, K., Ito, A., Beerling, D. J., Cadule, P., Ciais, P., Clark, D. B., Falloon, P., Friend, A.
549 D., Kahana, R., Kato, E., Keribin, R., Lucht, W., Lomas, M., Rademacher, T. T., Pavlick, R.,

550 Schaphoff, S., Vuichard, N., Warszawski, L., and Yokohata, T.: Quantifying uncertainties in
551 soil carbon responses to changes in global mean temperature and precipitation, *Earth Syst.*
552 *Dynam.*, 5, 197-209, doi:10.5194/esd-5-197-2014, 2014.

553 Phipps, S. J., L. D. Rotstayn, H. B. Gordon, J. L. Roberts, A. C. Hirst and W. F. Budd: The
554 CSIRO Mk3L climate system model version 1.0 - Part 1: Description and evaluation,
555 *Geoscientific Model Development*, 4, 483-509, doi:10.5194/gmd-4-483-2011, 2011.

556 Sarmiento, J. L., Gloor, M., Gruber, N., Beaulieu, C., Jacobson, A. R., Mikaloff Fletcher, S.
557 E., Pacala, S. and Rodgers, K.: Trends and regional distributions of land and ocean carbon
558 sinks, *Biogeosciences*, 7(8), 2351–2367, doi:10.5194/bg-7-2351-2010, 2010.

559 Tarnocai, C., Canadell, J. G., Schuur, E. a. G., Kuhry, P., Mazhitova, G. and Zimov, S.: Soil
560 organic carbon pools in the northern circumpolar permafrost region, *Glob. Biogeochem.*
561 *Cycles*, 23(2), GB2023, doi:10.1029/2008GB003327, 2009.

562 Taylor, K. E., Stouffer, R. J. and Meehl, G. A.: An Overview of CMIP5 and the Experiment
563 Design, *Bull. Am. Meteorol. Soc.*, 93(4), 485–498, doi:10.1175/BAMS-D-11-00094.1, 2012.

564 Todd-Brown, K. E. O., Randerson, J. T., Hopkins, F., Arora, V., Hajima, T., Jones, C.,
565 Shevliakova, E., Tjiputra, J., Volodin, E., Wu, T., Zhang, Q., and Allison, S. D.: Changes in
566 soil organic carbon storage predicted by Earth system models during the 21st century,
567 *Biogeosciences*, 11, 2341-2356, doi:10.5194/bg-11-2341-2014, 2014.

568 Todd-Brown, K. E. O., Randerson, J. T., Post, W. M., Hoffman, F. M., Tarnocai, C., Schuur,
569 E. A. G., and Allison, S. D.: Causes of variation in soil carbon simulations from CMIP5 Earth
570 system models and comparison with observations, *Biogeosciences*, 10, 1717-1736,
571 doi:10.5194/bg-10-1717-2013, 2013.

572 Todd-Brown, K. E. O., Hopkins, F. M., Kivlin, S. N., Talbot, J. M. and Allison, S. D.: A
573 framework for representing microbial decomposition in coupled climate models,
574 *Biogeochemistry*, 109(1), 19–33, doi:10.1007/s10533-011-9635-6, 2012.

575 Wang, Y. P., Kowalczyk, E., Leuning, R., Abramowitz, G., Raupach, M. R., Pak, B., Gorsel,
576 E. van and Luhar, A.: Diagnosing errors in a land surface model (CABLE) in the time and
577 frequency domains, *J. Geophys. Res.*, 116, G01034, doi:10.1029/2010JG001385, 2011.

578 Wang, Y. P., Law, R. M. and Pak, B.: A global model of carbon, nitrogen and phosphorus
579 cycles for the terrestrial biosphere, *Biogeosciences*, 7(7), 2261–2282, doi:10.5194/bg-7-2261-
580 2010, 2010.

581 Wania, R., Meissner, K. J., Eby, M., Arora, V. K., Ross, I., and Weaver, A. J.: Carbon-
582 nitrogen feedbacks in the UVic ESCM, *Geosci. Model Dev.*, 5, 1137-1160, doi:10.5194/gmd-
583 5-1137-2012, 2012.

584 Wieder, W. R., Bonan, G. B and Allison, S. D., Global soil carbon projections are improved
585 by modelling microbial processes, *Nature Clim. Change* 3, 909–912,
586 doi:10.1038/nclimate1951, 2013.

587 Xenakis, G. and Williams, M., Comparing microbial and chemical approaches for modelling
588 soil organic carbon decomposition using the DecoChem v1.0 and DecoBio v1.0 models,
589 *Geosci. Model. Dev. Discuss.*, 7, 33-72, doi:10.5194/gmdd-7-33-2014, 2014.

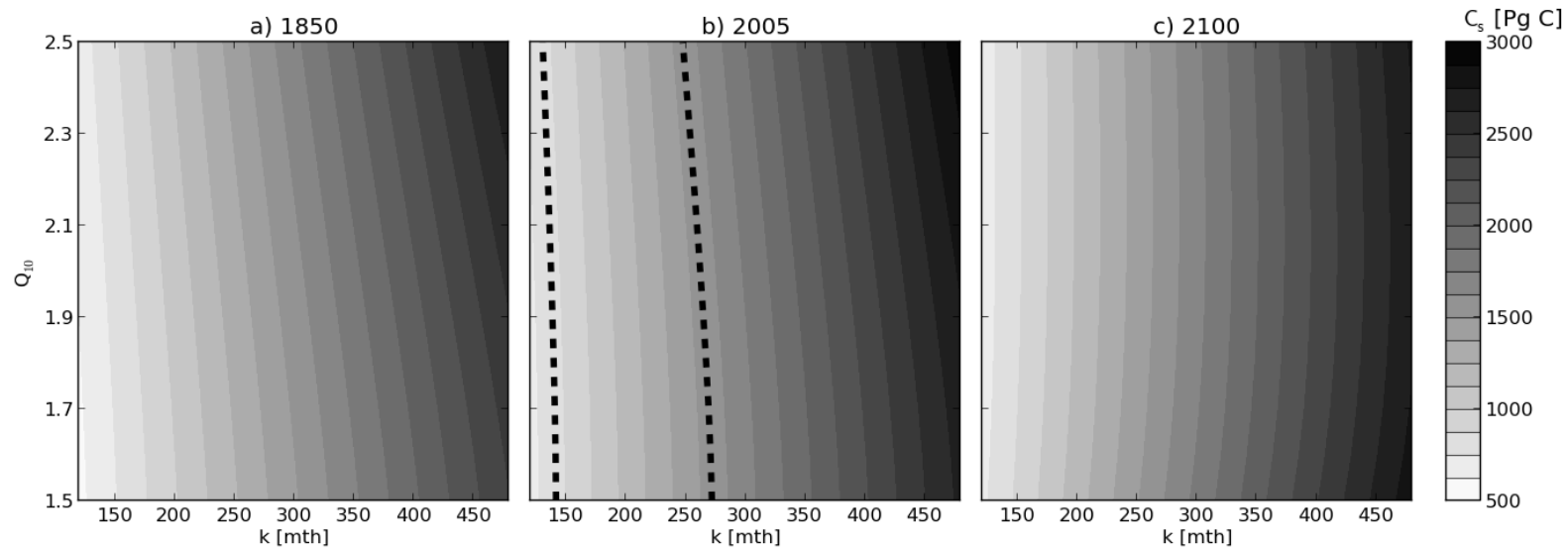
590 Xia, J. Y., Luo, Y. Q., Wang, Y.-P., Weng, E. S., and Hararuk, O.: A semi-analytical solution
591 to accelerate spin-up of a coupled carbon and nitrogen land model to steady state, *Geosci.*
592 *Model Dev.*, 5, 1259-1271, doi:10.5194/gmd-5-1259-2012, 2012.

593 Xia, J., Luo, Y., Wang, Y.-P. and Hararuk, O.: Traceable components of terrestrial carbon
594 storage capacity in biogeochemical models. *Glob. Change Biol.*, 19, 2104–2116. doi:
595 10.1111/gcb.12172, 2013.

596 Zhang, Q., Wang, Y. P., Pitman, A. J. and Dai, Y. J.: Limitations of nitrogen and
597 phosphorous on the terrestrial carbon uptake in the 20th century, *Geophys. Res. Lett.*, 38,
598 L22701, doi:10.1029/2011GL049244, 2011.

599

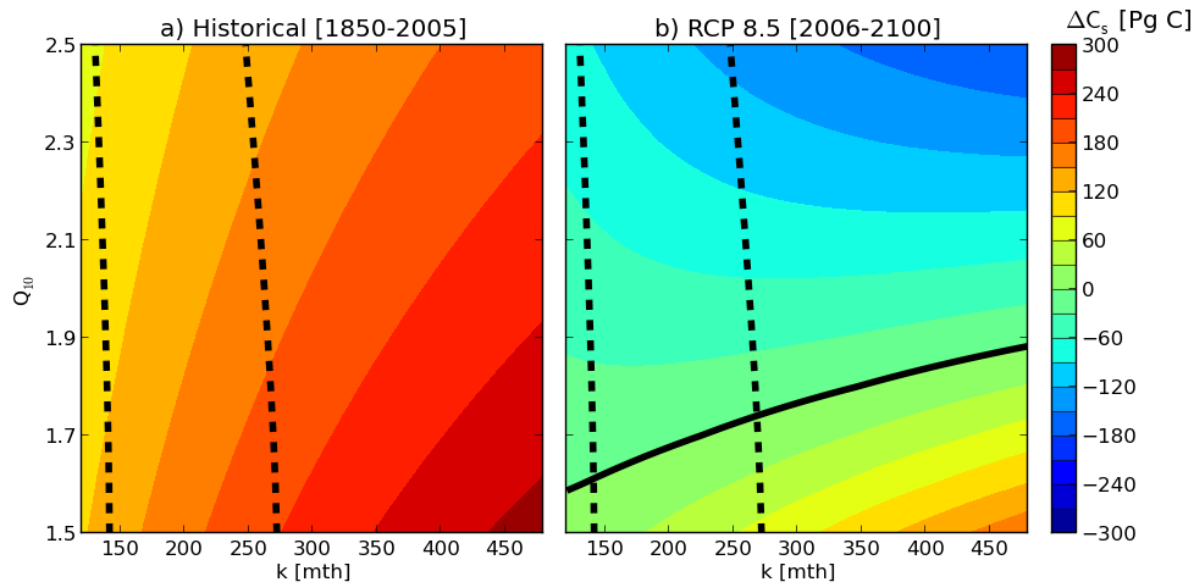
600



601

602 **Figure 1.** Snapshots of total soil carbon in the reduced complexity model as a function of parameter values. Dashed contours in panel b indicate
 603 the CI₉₅ of the HWSD in 2005 (830 – 1550 Pg C).

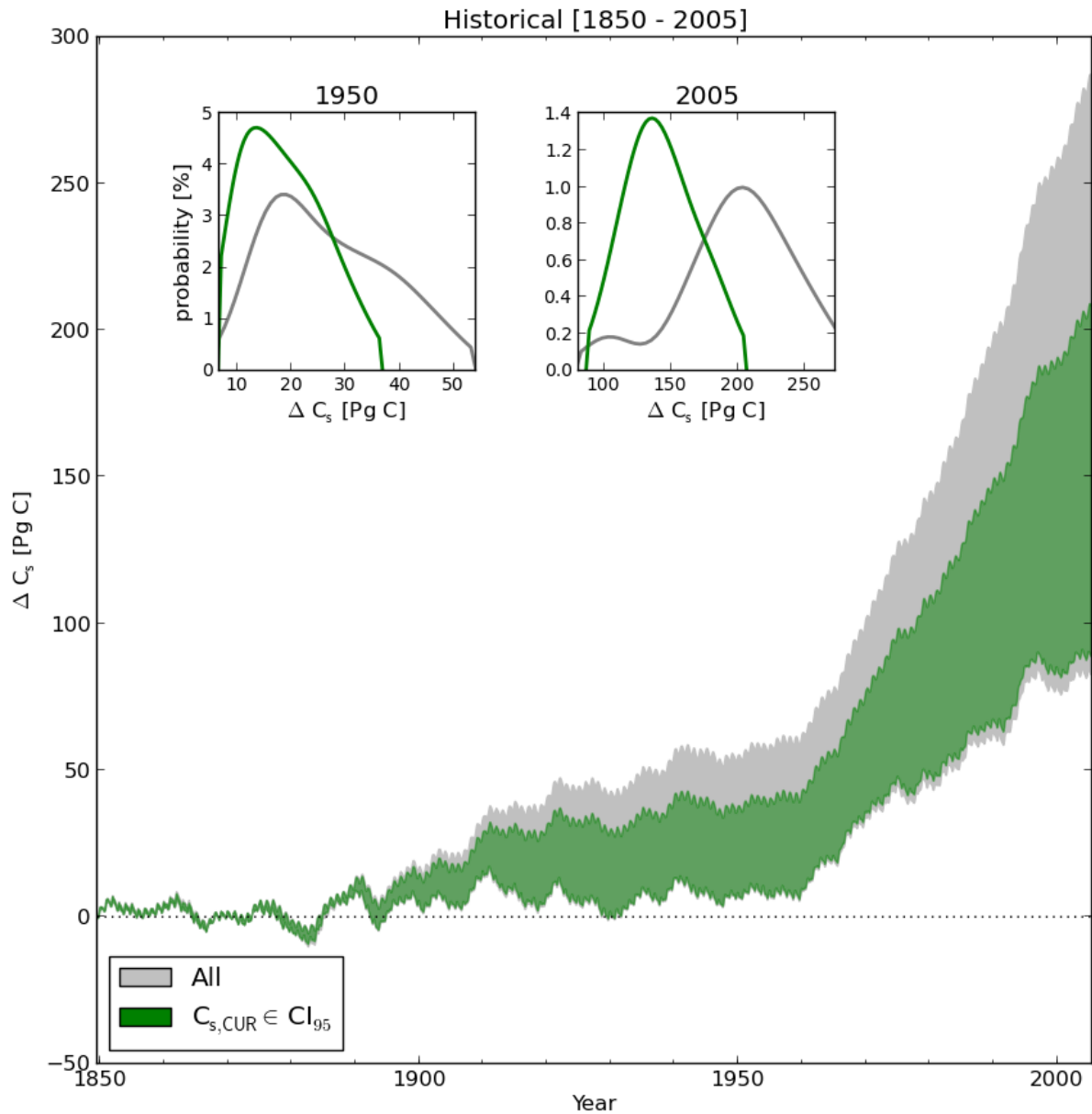
604



605

606 **Figure 2.** Change in total soil carbon in the reduced complexity model as a function of parameter values for each period as indicated. Dashed
 607 contours in panel b indicate model versions that produced soil stocks within the CI_{95} of the HWSD in 2005 (830 – 1550 Pg C). The thick black
 608 line represents no change.

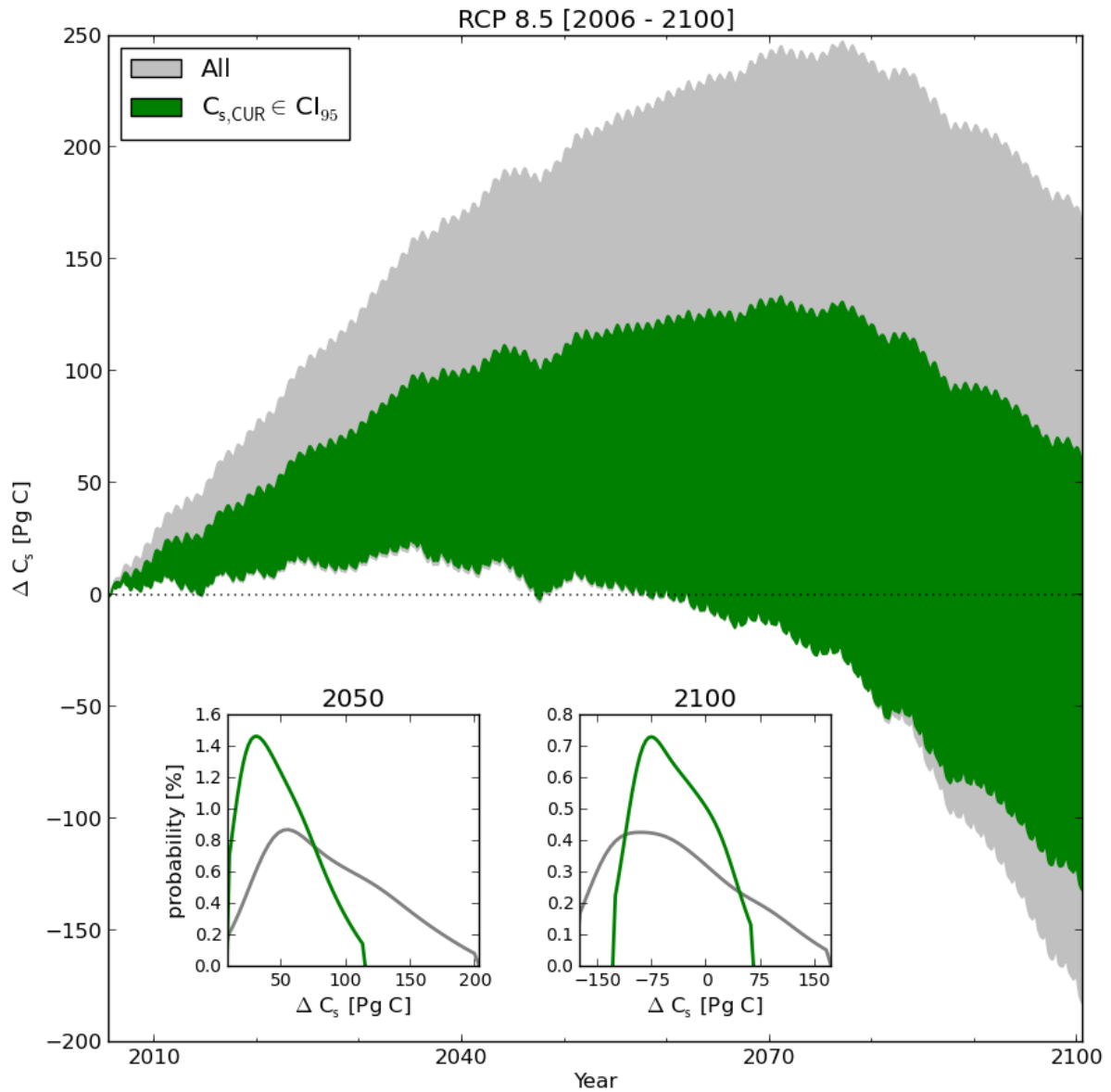
609



610

611 **Figure 3.** Change in total soil carbon through time for historical simulations. Insets represent
 612 the probability density function of the change since 1850 for the period indicated. Grey is for
 613 all simulations while green is used to distinguish simulations for which total soil carbon is
 614 within the CI_{95} of the HWSD in 2005.

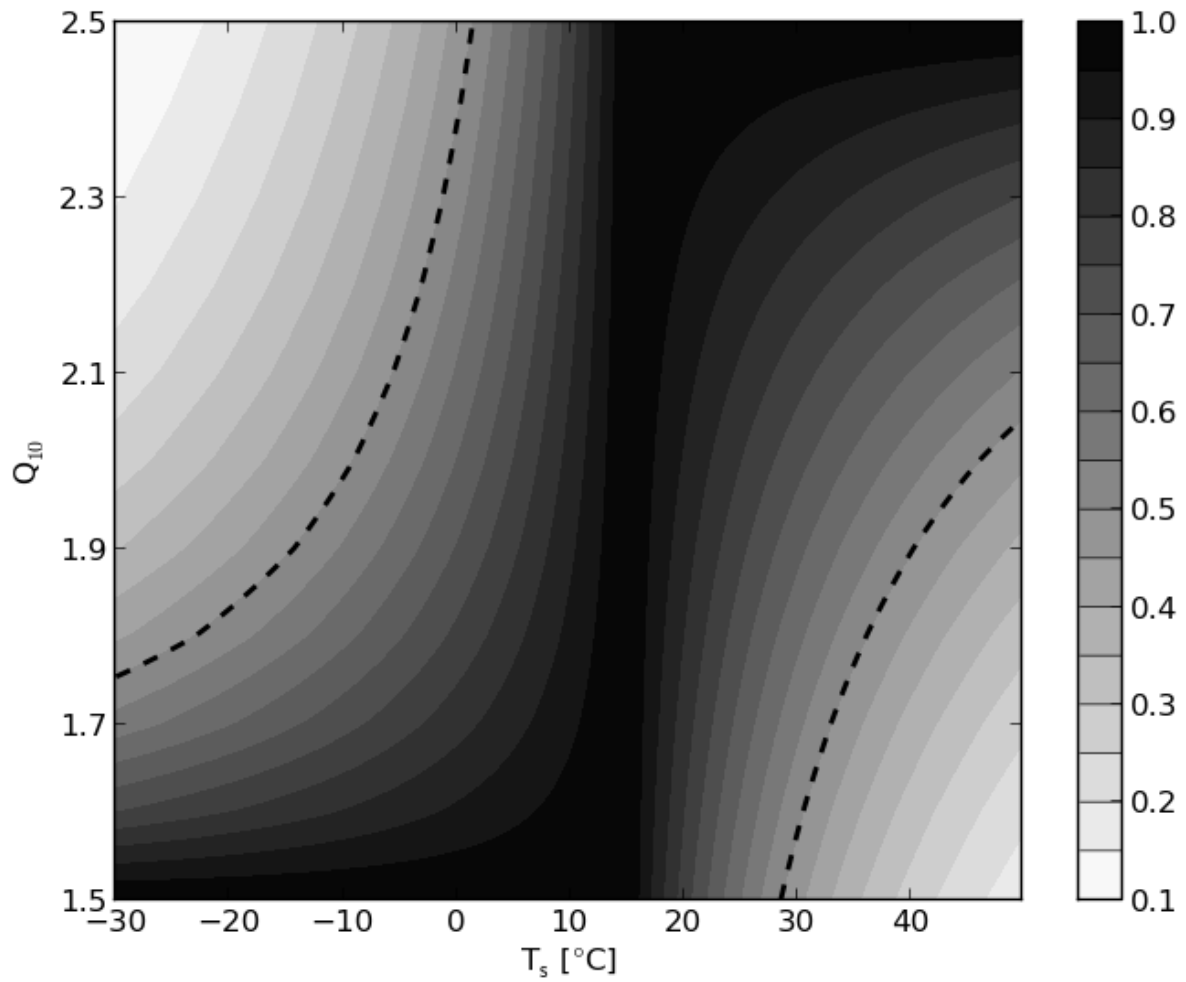
615



616

617 **Figure 4.** Change in total soil carbon through time for RCP 8.5 projections. Insets represent
 618 the probability density function of the change since 2005 for the indicated year. Grey is for
 619 all simulations while green is used to distinguish simulations for which total soil carbon is
 620 within the CI_{95} of the HWSD in 2005.

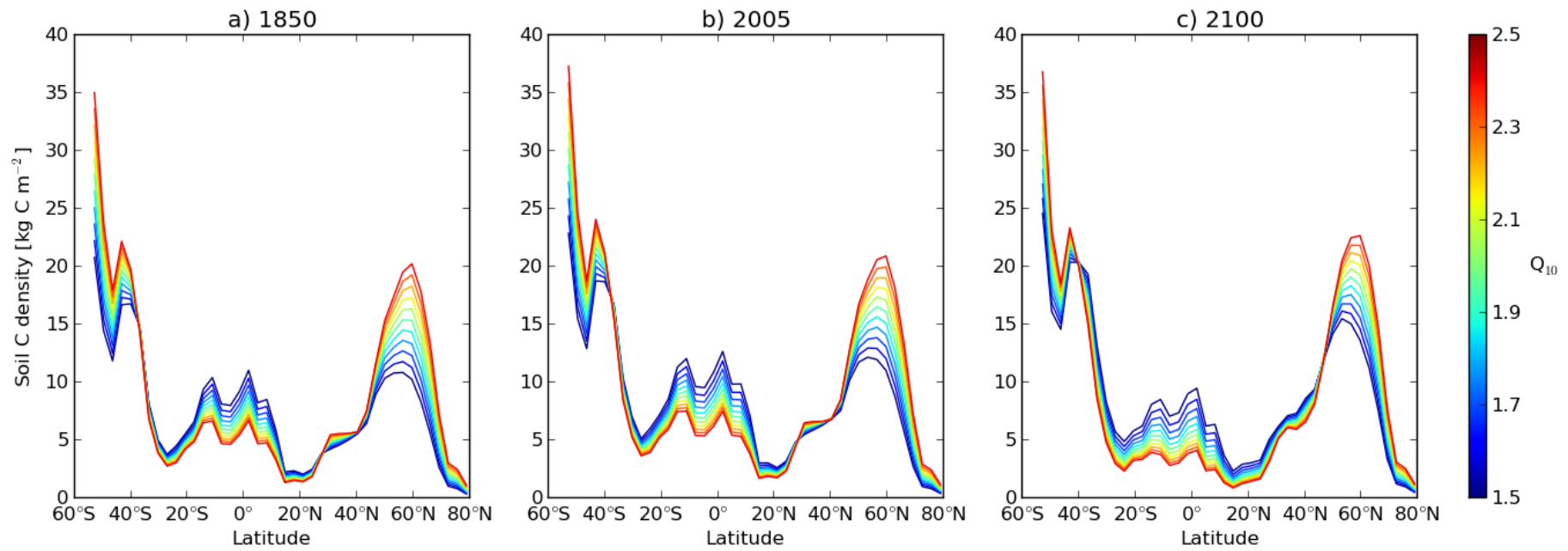
621



622

623 **Figure 5.** Values of f_T as a function of T_s and Q_{10} . For each temperature, the value is
 624 expressed as the proportion of the maximum value achieved for any value of Q_{10} . Areas
 625 outside of the dashed lines represent where f_T is less than 50% of the maximum for the same
 626 temperature.

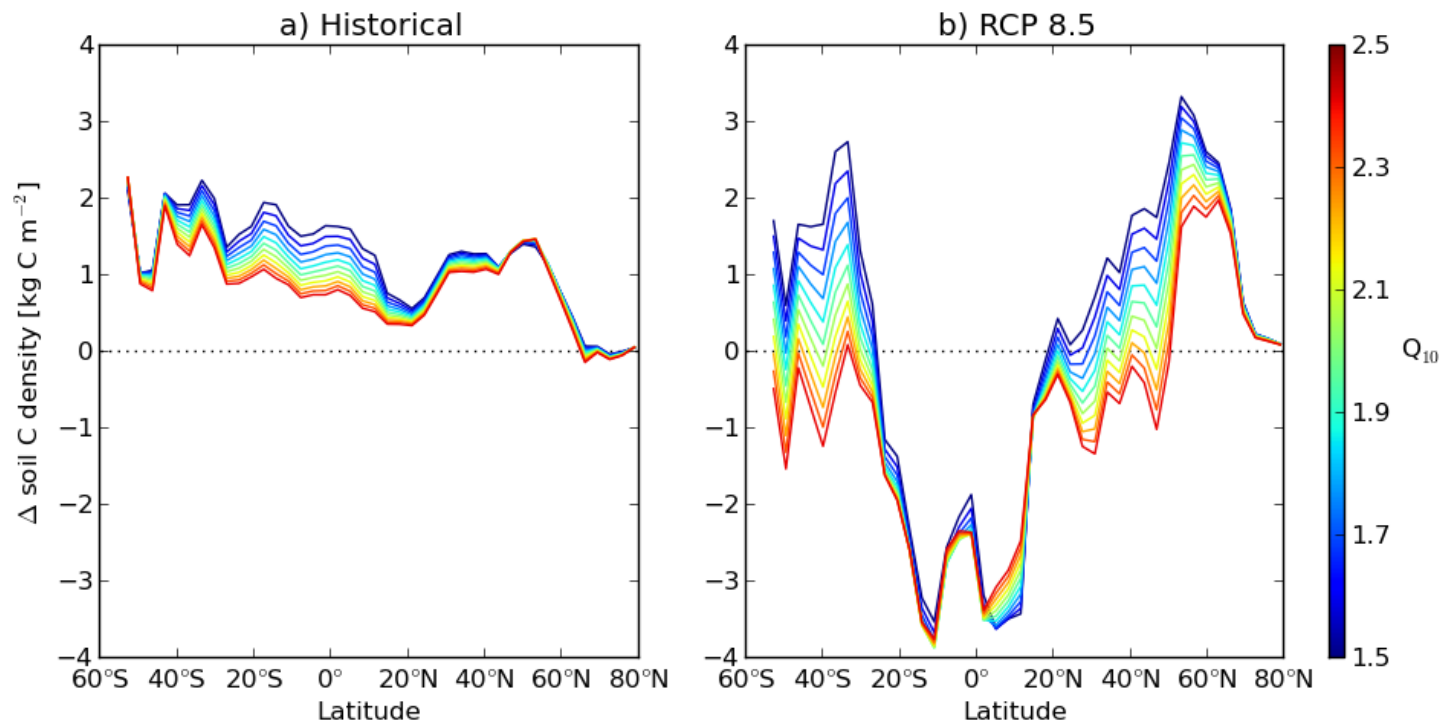
627



628

629 **Figure 6.** Zonal average soil carbon density in the reduced complexity model with $k=180$ months and various values of Q_{10} as indicated by the
 630 colour bar.

631



632

633 **Figure 7.** Zonal change in soil C density during historical simulations (a) and RCP8.5 (b)

634

635